

Liquid Crystal based adaptive optics system to compensate both low and high order aberrations in a model eye

Quanquan Mu

State Key Lab of Applied Optics, Changchun Institute of Optics, Fine Mechanics and Physics,
Chinese Academy of Sciences, Changchun, Jilin, 130033, China
Graduate School of the Chinese Academy of Sciences, Beijing, 100039, China
muquanquan@ciomp.ac.cn

Zhaoliang Cao, Dayu Li, Lifa Hu, and Li Xuan

State Key Lab of Applied Optics, Changchun Institute of Optics, Fine Mechanics and Physics,
Chinese Academy of Sciences, Changchun, Jilin, 130033, China

Abstract: Based on a simple eye model system, a high resolution adaptive optics retina imaging system was built to demonstrate the availability of using liquid crystal devices as a wave-front corrector for both low and high order aberrations. Myopia glass was used to introduce large low order aberrations. A fiber bundle was used to simulate the retina. After correction, its image at different diopters became very clear. We can get a root mean square(RMS) correction precision of lower than 0.049λ ($\lambda = 0.63\mu\text{m}$) for over to 10 diopters and the modulation transfer function (MTF) retains 51lp/mm, which is nearly the diffraction limited resolution for a 2.7mm pupil diameter. The closed loop bandwidth was nearly 4 Hz, which is capable to track most of the aberration dynamics in a real eye.

©2007 Optical Society of America

OCIS codes: (230.3720) Liquid-crystal devices; (010.1080) Adaptive optics; (330.4460) Ophthalmic optics

References and links

1. H. W. Babcock, "The possibility of compensating astronomical seeing," *Publ. Astron. Soc. Pac.* **65**, 229-236 (1953).
2. M. S. Smirnov, "Measurement of wave aberration in the human eye," *Biophysics* **6**, 766-795 (1961).
3. A. W. Dreher, J. F. Bille, and R. N. Weinreb, "Active optical depth resolution improvement of the laser tomographic scanner," *Appl. Opt.* **24**, 804-808 (1989).
4. J. Liang, B. Grimm, S. Goelz, and J. Bille, "Objective measurement of the wave aberrations of the human eye with the use of a Hartmann-Shack wave-front sensor," *J. Opt. Soc. Am. A* **11**, 1949-1957 (1994).
5. J. Liang, D. R. Williams, and D. T. Miller, "Supernormal vision and high-resolution retinal imaging through adaptive optics," *J. Opt. Soc. Am. A* **14**, 2884-2892 (1997).
6. J. Carroll, D. C. Gray, A. Roorda, and D. R. Williams, "Recent advances in Retinal Imaging with Adaptive Optics," *Opt. Photonics News* **16**, 36-42 (2005).
7. Z. Cao, L. Xuan, L. Hu, Y. Liu, and Q. Mu, "Effects of the space-bandwidth product on the liquid-crystal kinoform," *Opt. Express* **13**, 5186-5191 (2005).
8. L. Hu, L. Xuan, Y. Liu, Z. Cao, D. Li, and Q. Mu, "Phase-only liquid crystal spatial light modulator for wave-front correction with high precision," *Opt. Express* **12**, 6403-6409 (2004).
9. F. V. Martin, P. M. Prieto, and P. Artal, "Correction of the aberrations in the human eye with a liquid-crystal spatial light modulator: limits to performance," *J. Opt. Soc. Am. A* **15**, 2552-2562 (1998).
10. Q. Mu, Z. Cao, L. Hu, D. Li, and L. Xuan, "Adaptive optics imaging system based on a high-resolution liquid crystal on silicon device," *Opt. Express* **14**, 8013-8018 (2006).
11. E. J. Fernandez, I. Iglesias, and P. Artal, "Closed-loop adaptive optics in the human eye," *Opt. Lett.* **26**, 746-748 (2001).
12. L. N. Thibos and A. Bradley, "Use of Liquid-Crystal Adaptive-Optics to alter the refractive state of the eye," *Optom. Vision Sci.* **74**, 581-587 (1997).
13. P. M. Prieto, E. J. Fernandez, S. Manzanera, and P. Artal, "Adaptive optics with a programmable phase modulator: applications in the human eye," *Opt. Express* **12**, 4059-4071 (2004).

14. K. Bessho, T. Yamaguchi, N. Nakazawa, T. Mihashi, Y. Okawaa, N. Maeda, and T. Fujikado, "Live photoreceptor imaging using a prototype adaptive optics fundus camera: A preliminary result," *Invest. Ophthalmol. Vis. Sci.* **46**, 3547 Suppl. S (2005).
 15. E. J. Fernandez, B. Povazay, B. Hermann, A. Unterhuber, H. Sattmann, P. M. Prieto, R. Leitgeb, P. Ahnelt, P. Artal, and W. Drexler, "Three-dimensional adaptive optics ultrahigh-resolution optical coherence tomography using a liquid crystal spatial light modulator," *Vision Res.* **45**, 3432-3444(2005).
 16. T. Shirai, "Liquid-crystal adaptive optics based on feedback interferometry for high-resolution retinal imaging," *Appl. Opt.* **41**, 4013-4023(2002).
 17. Y. Liu, Z. Cao, D. Li, Q. Mu, L. Hu, X. Lu, and L. Xuan, "Correction for large aberration with phase-only liquid-crystal wavefront corrector," *Opt. Eng.* **45**, 128001(2006).
-

1. Introduction

Adaptive optics, an active technique, was first suggested by Babcock in astronomy to improve the performance of ground-based telescopes [1]. After this success, it was expanded to several fields and showed its availability. In 1961, Smirnov first suggest to improve the optical performance of the eye by correction of its optical aberrations [2]. At the beginning, only some kinds of low order aberrations at a small value level could be corrected using a deformable mirror [3]. In 1994, Liang et al. introduced the Hartmann-Shack wave-front sensor for measuring the aberration of eye up to 10th order [4]. Based on this technique, they successfully build an adaptive optics system for high-resolution retinal imaging and proved the possibility of supernormal vision [5]. High-resolution retinal imaging has found a home in vision science, where it is used by a number of researchers to further our understanding of the human retina [6]. In most cases the compensation device used was deformable mirror. Both conventional deformable mirror and micromachined membrane deformable mirror, suffered from low actual density and small strokes, which restricted the performance of adaptive optics in retina imaging. Liquid crystal based compensator may be a suitable device for retina imaging because of its low cost, low power consumption, high pixel density and especially larger modulation depth [7, 8]. Previous works have demonstrated the feasibility but haven't showed the advantage of liquid crystal due to its small pixel density [9]. Based on a high-resolution LCOS device, we have built an adaptive optics system in former works, demonstrated its possibility to get a very high wave-front correction precision. Furthermore it can get a very large modulation depth after the use of phase wrapping technique [10].

Most kind of adaptive optics retina imaging systems only correct high order aberrations in the human eye to improve the imaging performance. Low order aberrations are often very large and deformable mirror has not such a high stroke. Usually, a four mirror sub system was used to correct the defocus of eye, which makes the whole system complex and could not fully correct these low order aberrations like defocus and astigmatism, which were always large [11]. Thibos et al. has reported about the correction of spherical and astigmatic refractive changes in the eye with only about 1.5 diopters with a 127 liquid crystal cells [12]. It showed the possibility of using liquid crystal device to alter the refractive states in the eye although still too restricted. After that, other liquid crystal based adaptive optics systems still compensate high order aberrations only. Prieto et al. implemented a liquid crystal-based adaptive optics system for close-loop correction of ocular aberrations, discussed its potential and checked its performance in both artificial and real eyes, showed the possibility of using liquid crystal devices as a high-resolution wave-front corrector even in an open-loop configuration [13]. Bessho et al. showed some preliminary results on high resolution fundus imaging using a liquid crystal modulator to correct the ocular aberrations [14]. Fernandez et al. has developed an adaptive optics OCT system which includes a liquid crystal phase modulator and obtained high resolution tomograms of the live retina [15]. Another Liquid-crystal adaptive optics system based on feedback interferometry was introduced by Shirai who proposed a system for high-resolution retinal imaging using an interferogram-driven liquid crystal modulator [16]. In this paper, we used a high-resolution LCOS device in a modeled retina imaging adaptive optics system for both low and high order aberrations correction. Based on its high pixel density and small pixel pitch, the phase wrapping technique can be used to expand the modulation depth of the LCOS device. It is suitable for large range low

order wave-front error correction besides high order aberrations. This is benefit for retina imaging.

2. Apparatus

The LCR2500 LCOS device from Holoeye Corporation is used here. It can reach a total 2.2π phase stroke without phase wrapping at wavelength $0.6328\mu\text{ m}$. With the phase wrapping technique, which is like the binary optics, we can get a larger modulation depth. we assume that the quantization for one wavelength use at least 8 steps, which related to a over 90% diffraction efficiency for binary optics, then the maximum phase stroke will be up to 200π for tilt and 100π for defocus on the whole device. A Shack-Hartmann sensor (HASO32, Imagine Optic) was used to measure the wave-front error of the model eye. The detail parameters for both of them are showed in table 1.

Table 1. Detail parameters of LCR2500 and HASO32

(a) LCR2500		
Parameter	Value	Unit
Active area dimensions	19.5x14.6	mm
Display resolution	1024 (H) x 768 (V)	pixels
Pixel pitch	19 x19	μm
Gray Levels	256 (8 bit)	
Optical efficiency:	> 75%	
Reflectance		
Aperture ratio	> 93%	
Liquid crystal type	45° twisted nematic	
Max. refresh frame rate	75	Hz
Cell gap	5.5	μm

(b) HASO32		
Parameter	Value	Unit
Aperture dimension	5 x 5	mm^2
Number of sub-apertures	32 x 32	
Tilt dynamic range	$>\pm 3(520\lambda)$	$^\circ$
Focus dynamic range	$\pm 0,025$ to $\pm \infty$ (200λ)	m
Repeatability (rms)	$<1/200$	wavelength
Spatial resolution	~ 160	μm
Max acquisition frequency	77	Hz

3. Optical configuration

A simple eye model was build at first as shown in Fig. 1. It consists of a fiber bundle, an achromatic cemented double lens and a diaphragm which represent the retina, the lens and the pupil respectively. The focal length we used here is 60mm, which is approximately twice the focal length of real human eye. The pupil diameter is 2.7mm. The diameter of the fiber bundle is 1mm and the diameter for each fiber is $25\mu\text{ m}$. At this configuration we can get a diffraction limited resolution of nearly $17.16\mu\text{ m}$ at the focus point of the lens, which is comparable with the diameter of the fiber we used. So it is convenient for us to check whether it reached the diffraction limited resolution or not after the correction. The purpose of this study is to explore the availability of the LCOS device in retina imaging to correct both low and high order aberrations. A 633nm monochromatic light, which was produced by a white light source attached with a 633nm filter, emitted out from the fiber bundle directly to model

the retina been illuminated. The light power emitted from the model eye is at a level of 9μ w. The power density is 157μ w/cm² which is ten times bigger than the maximum permissible exposure limits for continues exposure for a real eye. The illumination optical system and the safe power for a real eye will be considered in future works. Based on this eye model, we constructed an adaptive optics retina imaging system uses the LCR2500 to correct the wavefront errors induced by myopia glass and the roughness of the LCOS device.

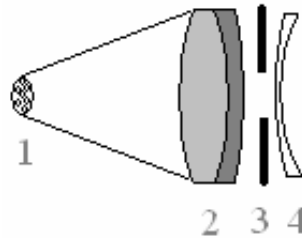


Fig. 1. Eye model (1. fiber bundle; 2. double lens; 3. diaphragm; 4. myopia glass)

Figure 2 shows the schematic diagram of the adaptive optics retina imaging system. Light emitted out from the eye model was refocused by lens L1 which has the same focal length as the eye model. Then it became horizontally polarized after passing through the polarizer P. The linearly polarized light was collimated by lens L2 before projected onto the LCOS. The L1 and L2 lenses pair also makes sure the LCOS plane is conjugated with the pupil. In the same way, the L2 and L3 conjugated the LCOS to the plane of L4, and then conjugated with the microlens array of the HASO by L5. The CCD camera recorded the retina image at the focus of the lens L4. A hole was used here to reject unwanted light from the system. The actual area on the LCOS we used here was approximately 14mm in diameter based on the zoom effect of L1 and L2. Optical layout in lab is shown in Fig. 3.

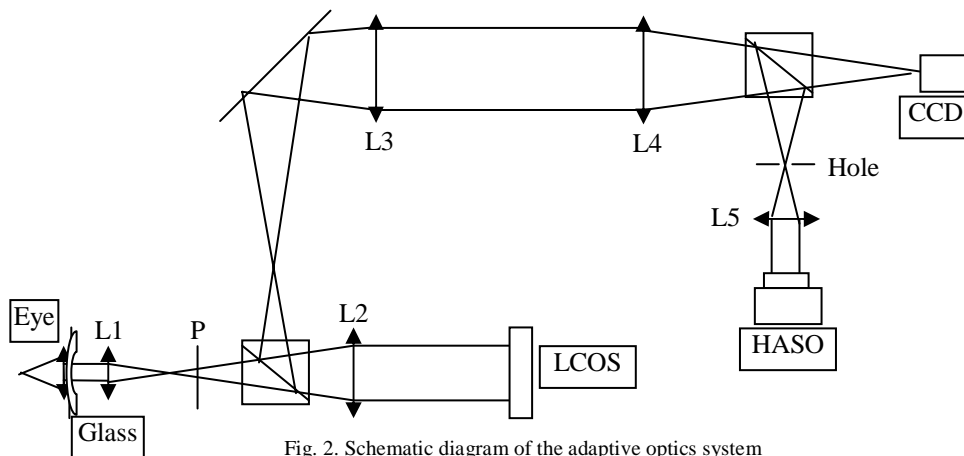


Fig. 2. Schematic diagram of the adaptive optics system

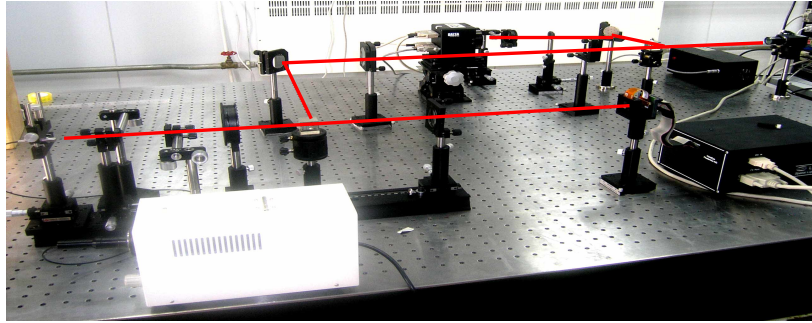


Fig. 3. Optical layout in lab

4. Results and discussion

Myopia glasses with different diopters are inserted directly after the pupil to induce large wave-front aberrations in order to evaluate the ability of using LCOS device in retina imaging to correct both low and high order aberrations. We used five glasses from 5 diopters to 15 diopters in this experiment. Wave-front aberrations for different diopters in root mean square (RMS) showed in Fig. 4. The RMS value of 0.788λ at zero diopter represents the aberration of the artificial eye. It includes both low and high order aberrations induced by the whole system and the roughness of the LCOS device. In Fig. 5 the theory value of the wave-front error in RMS was compared with the experimental data. The theory value is considered as the sum of the roughness of the optical system at OD condition and the RMS value related to the diopters we induced. The distance between the myopia glass and the pupil plane is nearly 4mm. We can see that they matched each other very well when the diopter was lower than 10D. Along with the increase of diopter it induced the fiber image at the hole position enlarged, which can be seen by the CCD camera showed in Fig. 6. So some light may be rejected by the hole, which will reduce the detected wave-front aberrations. When the diopter was larger than 10 diopters, due to the rejection action, the distinction of wave-front error between theory and experiment showed obviously.

Wave-front aberrations detected by HASO were larger than one wavelength. Here we used the “phase wrapping” technique, which has been introduced in detail in previous works from us [17] and others [12], to enlarge the modulation depth of the LCOS device. Due to the zoom effect of lenses L2, L3, L4 and L5, every microlens of the HASO corresponds to nearly 24×24 LCOS pixels. So there is no piston or discontinuous phase affect on the slope measurement of the wave-front aberration. After the detection of HASO, the conjugated wave-front was reconstructed and modulo 2π by computer before converted it into grey scales. Then, it was sent to the LCOS. The whole system works in a closed-loop feedback configuration.

Images of the fiber bundle were recorded before and after wave-front correction. Figure 6 showed the images for different diopters before correction. We can see it blurred and enlarged significantly along with the increase of diopters. After correction, they all became more clear than before. Also we can see that the definition of the image decreased obviously when the diopter larger than 12D. The same result supported by the modulation transfer function (MTF) curve in Fig. 8.

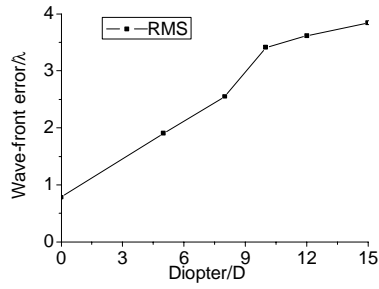


Fig. 4. Wave-front errors of the model eye for different diopters.

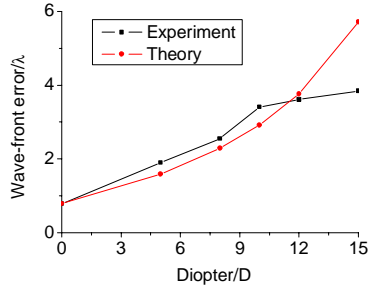


Fig. 5. Comparison of the wave-front errors of the model eye between theory and experiment in RMS.

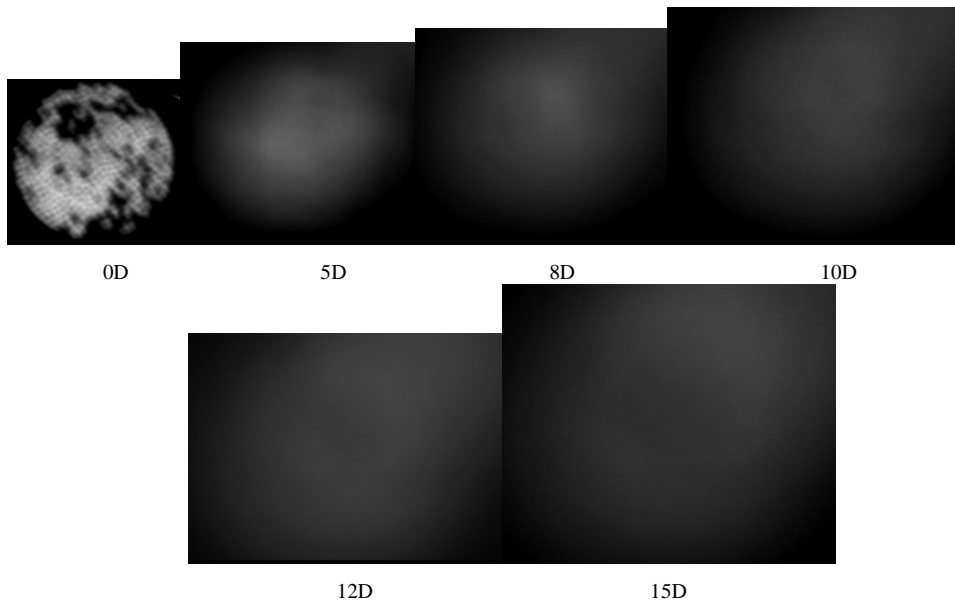


Fig. 6. Images of fiber bundle before wave-front correction for different diopters.

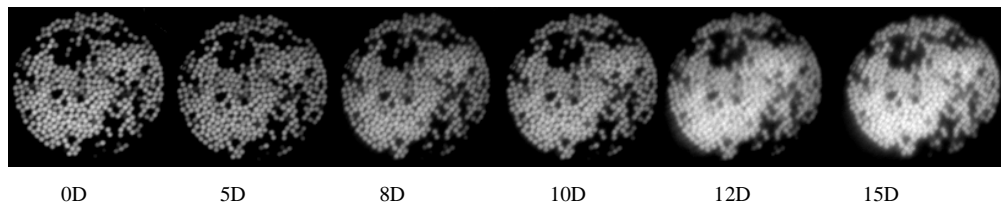


Fig. 7. Images of fiber bundle after wave-front correction for different diopters.

The critical frequency was defined where the MTF value equal to 0.1. Figure 9 showed the critical frequency after correction at different diopters. We can see it changes slightly when the diopter was lower than 10 diopters and it retains a resolution over 51lp/mm, which is nearly the diffraction limited resolution. The residual wave-front error in RMS increased slightly from lower than 0.02λ to nearly 0.049λ for over 10 diopters as shown in Fig. 10. This degradation mainly induced by the misalignment of myopia glass with the whole system and the influence of light rejected by the hole, which may reduce the precision of HASO. Further optimization will be done to improve its performance.

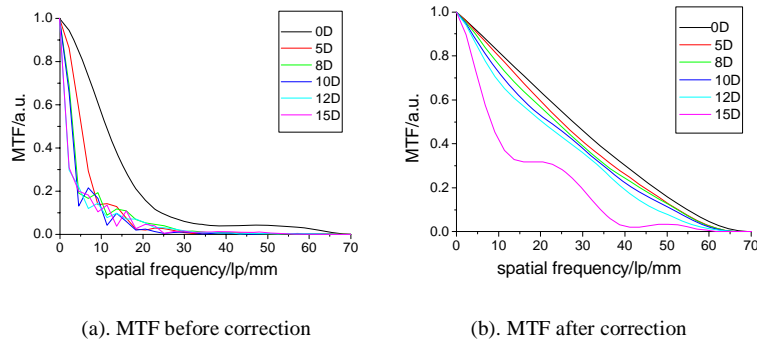


Fig. 8. MTF curve of the whole system for different diopters before and after correction

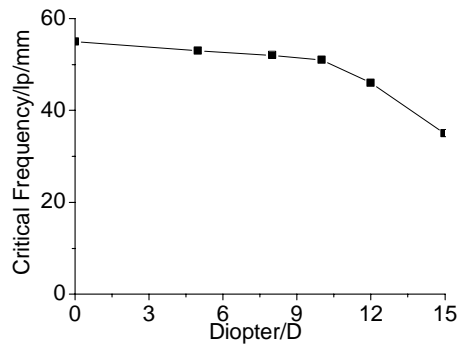


Fig. 9. The Critical frequency of the whole system for different diopters after correction.

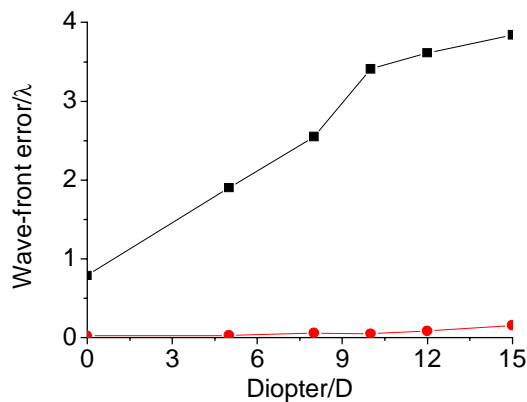


Fig. 10. RMS wave-front error of the model eye before (black) and after (red) correction

5. Conclusion

An adaptive optics retina imaging system has been built based on a simple eye model. A LCOS device was used to correct both low and high order aberrations simulated by myopia glass and the roughness of LCOS respectively. We can get a nearly diffraction limited resolution of 51lp/mm when the wave-front aberration is not more than 10 diopters and the correction precision in RMS remains lower than 0.049λ . All of this demonstrated that liquid crystal devices, which have high pixel density and very small pixel pitch, are very comfortable for large aberration correction. Also there are still a lot of works to improve its performance and used to a real human eye.

Acknowledgments

This work is supported by National Natural Science Foundation (No. 60578035, No. 50473040) and Science Foundation of Jilin Province (No. 20050520, No. 20050321-2).